Reduction of CO Emissions in the Environment by Preheating the Air in a Combustion Chamber

A. Boukhari[1], M.E.H. Attia[2,*], Z. Driss[3]

[1]Department of Mechanical Engineering, Faculty of Technology, University of El-Oued, 39000 El-Oued, Algeria.
[2]Department of Physics, Faculty of Science, University of El Oued, 39000 El Oued, Algeria.
[3]Laboratory of Electro-Mechanic Systems (LASEM), ENIS, University of Sfax, Tunisia.

*Corresponding author: attiameh@gmail.com; Tel.: +213 662524720

ARTICLE INFO

ABSTRACT/RESUME

Abstract: *In this paper, we studied numerically the effect of the preheating temperature of air in a non-premixed cylindrical (3D) combustion chamber. Using the commercial CFD code FLUENT, the characteristic parameters of the reactive flow, namely the axial velocity, the temperature and the mass fraction of carbon monoxide CO, was calculated. The study of this phenomenon consists in using a special treatment of mathematical models. The considered approaches were used to overcome the closure of the equations of the aero-thermo-chemical balance. The main objective of this work is to study the behavior of these parameters following the variation of the air inlet temperature. The utility of this method is to facilitate combustion chamber operation and a significant reduction in carbon monoxide emission.The obtained results show that the variation of the air temperature presents a great effect on the studied parameters. We have found that the air inlet temperature T=750 K is the best solution for CO carbon monoxide emission.*

I. Introduction

All biological life needs external energy. The degree of dependence of human societies on energy differs as the climate, comfort and activity of each society. Energy exists in many forms. Today, the technology allows producing in large quantities, using all the possible resources (fossils, water, wind, sun ...). At the dawn of the twentieth century, energy remains a major challenge, at the political, economic, scientific and environmental levels. Global demand for energy has increased enormously in these decades. This prediction is published by the International Energy Agency (IEA) in 2007. It shows the recorded and future evolution of world energy demand from 1980 to 2030. These predictions are derived from a scenario based on a set of assumptions macroeconomic conditions, population trends, energy prices, government policies and technology. According to this prediction, energy demand will double by the year 2050 and oil is the most important and remains the appropriate energy source. The latter covers almost all the needs of the means of transport. In second place comes the oldest fuel, coal, which is used in thermal power stations and in many industries. Natural gas occupies the third position, it is especially useful in homes for heating and domestic needs. All these fuels are consumed by the combustion route [1].

Combustion is one of the most important processes in the transformation of energy, making it possible to convert the chemical energy contained in the fuels into heat. Combustion is necessary for transport, electric power generation, manufacturing processes, heating, etc. Despite the benefits of combustion, it remains the biggest polluter on our planet. In addition to heat, combustion produces emissions that are harmful to the environment. This pollution mainly results from gases and particles thrown into the air by motor vehicles, heating installations, thermal power plants and industrial installations. Pollutant emissions are oxides of carbon, sulfur and nitrogen, greenhouse gases, dust, radioactive particles, chemicals, dioxygen, etc. [2-6].

However, the exploitation of hydrogen energy reduces enormously harmful emissions, because its use in fuel cells produces a nature-friendly product, i.e. water, as a side effect, making this alternative energy environmentally benign and economically advantageous in the chart of its transportations and applications [7].

Preheating the air reduces fuel consumption. Milani and Saponaro [8] showed that the use of a thermal capacity to preheat the combustion air made is possible to halve fuel consumption compared with conventional combustion without heat recovery from Fumes. In practice, Katsuki and Hasegawa [9] argue that if this method were applied to all industrial furnaces in Japan, total national energy consumption would decrease by 5%.

The main objective of this work is to present a 3D aerothermic chemistry study in a non-premixed cylindrical combustion chamber fed by G27, where the mixture named G27 is based on 82% methane and 18% nitrogen. Starting with the injection of G27 and air at the same temperature equal to T=300 K. Then the fuel temperature is set at the previous value and the inlet air temperature is varied at T=300 K, T=500 K, T=750 K and T=900 K. Typical combustion parameters were calculated as axial velocity, temperature and mass fraction of carbon monoxide CO. The simulation was performed by the commercial CFD code FLUENT to resolve the mathematical models. The obtained results confirm that the preheating of the air has an impact on the combustion parameters.

II. Burner Configuration

The configuration of the studied system is shown in Figure 1. The configuration consists of a non-premixed cylindrical combustion chamber fed by two coaxial jets (G27/Air). This system were a radius R4=61.15 mm, and a length of L=1 m, is subjected under pressure of a value equal to 3.8 atm and to isothermal temperature walls T=500 K [10-13]. The central jet presents an internal radius R1=31.57 mm and an external radius R2=31.75 mm, in order to inject the fuel G27 with a speed equal to V1=92.78 cm/s at a constant temperature T1=300 K. The annular jet is an internal radius of R3=46.85 mm, which injects preheated air at a rate equal to V2=20.63 m/s at different temperatures equal to T2=300 K, 500 K, 750 K and 900 K. The radius and speed of the annular jet is considered to be a characteristic of the jet.
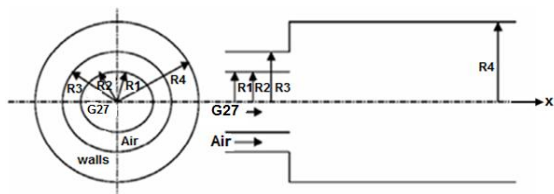

III. Mesh

Figure 2 shows sections of the used mesh for the simulation near the injection plane. The distribution of points and meshes is symmetrically presented on the control volume. The shape of the combustion chamber is cylindrical, the mesh used for the geometry is a hybrid mesh. The central part of the burner is meshed by prisms and the rest is meshed by rectangular parallelepipeds.

The mesh size of the combustion chamber is irregular because the flame may be located in any zone of the burner during the calculation. Indeed, since the phenomena of friction of the gases burned with the walls of the combustion chamber, there is the thermal effect of these isothermal walls. This unstructured mesh improves the quality of the results because it minimizes the dissipation of the numerical scheme. The zone of the injectors and the zones close to the walls are meshed more finely to take into account the gradients presented at this location consisting on:
• Gradients of mass fractions (layers of mixture of fuel and oxidant).
• Temperature gradients (thermal layer due to isothermal walls).
• Speed gradients (shear due to the jets of the injectors in the combustion chamber).

The mesh of the other zones of the burner is unrefined, since we have relatively increased the size of the cells.

The volume of control studied contains about 2,000,000 meshes, refined to some zones as already mentioned above, where the mesh size varies from $3.31\ 10^{-10}$ m^3 to $2.63\ 10^{-7}$ m^3 [13-16].

Figure 2. Mesh of the burner

IV. Governing Equations

The equilibrium equations of the aero-thermo-chemistry used for the combustion study with a compressible flow [10-16] are defined by the continuity equation:

The continuity equation is defined by:

$$\frac{\partial \bar{\rho}}{\partial t} + \frac{\partial}{\partial x_i}(\bar{\rho}\tilde{u}_i) = 0 \quad (1)$$

The momentum equations are written as follows:

$$\frac{\partial \bar{\rho}\tilde{u}_i}{\partial t} + \frac{\partial}{\partial x_i}(\bar{\rho}\tilde{u}_i\tilde{u}_j) = -\frac{\partial}{\partial x_i}[\bar{\rho}(\overline{u_i u_j} - \tilde{u}_i\tilde{u}_j)] - \frac{\partial \bar{p}}{\partial x_j} + \frac{\partial \bar{\tau}_{ij}}{\partial x_i} \quad (2)$$

Figure 1.Schematic of the burner

The energy equation is written as follows:

$$\frac{\partial}{\partial t}\bar{\rho}\tilde{h} + \frac{\partial}{\partial x_i}(\bar{\rho}\tilde{u}_i\tilde{h}) = -\frac{\partial}{\partial x_i}[\bar{\rho}(\overline{u_i h} - \tilde{u}_i\tilde{h})] + \frac{\partial \bar{p}}{\partial t} + \frac{\partial}{\partial x_i}u_j\bar{\tau}_{ij} \quad \textbf{(3)}$$

The species equations are written as follows:

$$\frac{\partial}{\partial t}\bar{\rho}\tilde{Y}_f + \frac{\partial}{\partial x_i}(\bar{\rho}u_i\tilde{Y}_f) = -\frac{\partial}{\partial x_i}[\bar{\rho}(\overline{u_i Y_f} - \tilde{u}_i\tilde{Y}_f)] + \bar{\dot{\omega}}_f \quad \textbf{(4)}$$

Where i = 1, 2, 3 and j = 1, 2, 3.
The thermodynamic state is written as follows:

$$\bar{p} = \bar{\rho}R_m\tilde{T} \quad \textbf{(5)}$$

In these equations, the unresolved Reynolds stresses $(\overline{u_i u_j} - \tilde{u}_i\tilde{u}_j)$ require a subgrid scale turbulence model. The unresolved species fluxes $(\overline{u_i Y_f} - \tilde{u}_i\tilde{Y}_f)$ and the enthalpy fluxes $(\overline{u_i h} - \tilde{u}_i\tilde{h})$ require a probability density function (PDF) approach. The filtered chemical reaction rate is characterized by $\bar{\dot{\omega}}_f$.

The LES models and the PDF approach explained and detailed in previous work [10-16].

V.   Results and Discussions

The equations of the balance sheet are solved by the finite volume method.

V.1.Axial velocity

The radial profiles of the mean axial velocity obtained by the numerical calculation are illustrated in Figure 3. However, the high velocity values are located in the area of the flame which is presented by the peaks in the two stations defined by x/R=0.14 and 0.38. The profiles show the same pattern, when the production of the mixing layer presented by the peaks is located approximately in the same position. The positions of the peaks move at the level of the jet of air. The curves represent the change of the mean axial velocity in a non-premixed cylindrical combustion chamber in terms of the radial distance in the various preceding stations. In these conditions, the fuel G27 is injected at a constant temperature equal to T=300 K. The considered air inlet temperature are equal to T=300 K, T=500 K, T=750 K and T=900 K. Indeed, it has been noted that the four curves are superimposed identically with a slight decrease. In fact, the average speed is not affected by the preheating of the air. In the case of the preheating with a temperature T=750 K, it should be noted that the extremum of the curve corresponds to an axial

velocity V=21.5 m/s and a position r/R=0.7 in the first case defined by x/R=0.14. In the second case defined by x/R=0.38, the extremum of the curve of variation of the speed corresponds to a value equal to V=20.5 m/s for a position equal to r/R=0.7.
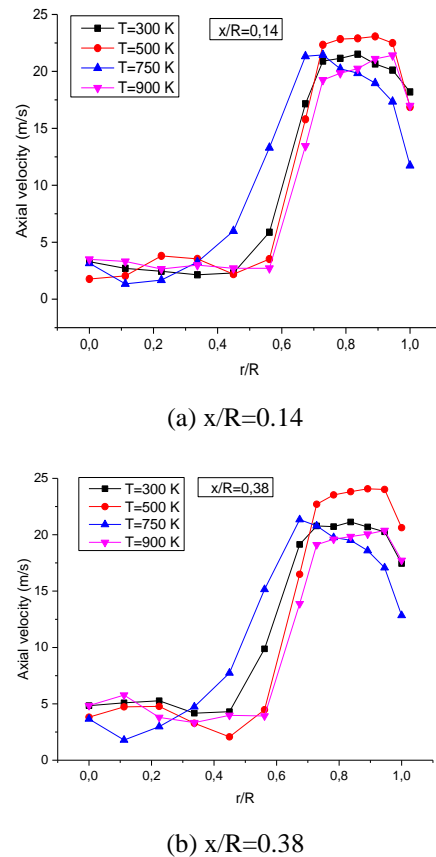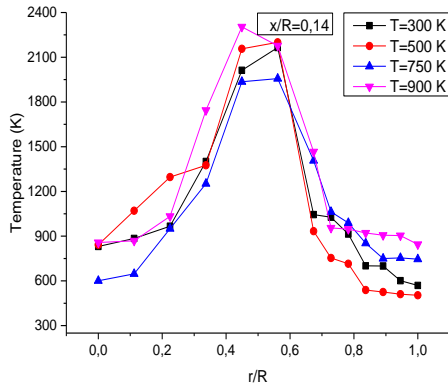

(a) x/R=0.14

(b) x/R=0.38

***Figure 3.*** *Radial profiles of the axial velocity*

V.2 .Temperature

The behavior of the temperature in the combustion chamber during the non-premixed combustion of G27 for different cases of air intake at T=300 K, T=500 K, T=750 K and T=900 K is presented in Figure 4 at two stations x/R=0.14 and 0.38. According to these results, the profiles have the same appearance. The highest temperature values are in the vicinity of the flame area. They begin to decrease when approaching to the walls of the burner whose temperature is equal to T=500 K. The zone of the flame is the zone of the chemical reaction of the CH_4 with the air, because the G27 fuel is based on 82% of the methane. Under these conditions, the heat source is generated by the chemical reactions caused by the breakdown of carbon bonds and hydrogen, which react with oxygen to produce CO_2, CO, H_2O and OH.

Moreover, it should be noted that the temperature in the four curves takes the same shape with different values. In the case of preheating with a temperature T=750 K, it should be noted that the extremum of the curve corresponds to a temperature T=1900 K and a position r/R=0.5 in the first case defined by x/R=0.14. In the second case defined by x/R=0.38, the extremum of the temperature variation curve corresponds to a value equal to T=2050 K for a position equal to r/R=0.5.

(a) x/R=0.14
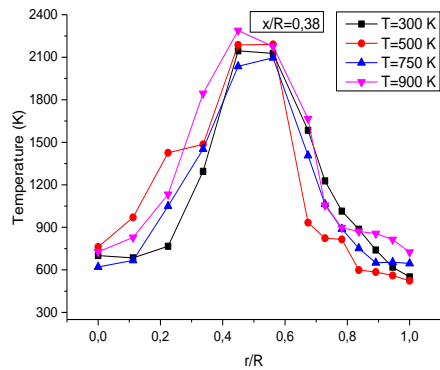
(b) x/R=0.38

Figure 4. *Radial profiles of the temperature*

V.3. CO Fraction Mass

In this section, we choose the carbon monoxide as a chemical species of pollutant. The carbon monoxide field is varied between two stations x/R=0.14 and 0.38. In Figure 5, the mass fraction of carbon monoxide 'CO' produced during the combustion of the fuel G27 is presented. The results show that the CO value are high in the middle of the combustion chamber and begins to decrease until reaching the value zero in the vicinity of the walls of the combustion chamber. Similarly, the CO values decrease when moving away from the combustion chamber inlet (flame area). The decrease in CO is due to secondary reactions with O_2 to become CO_2. The obtained results show that

the temperature behaves in the same way as the mass fraction of carbon monoxide CO. This means that the region of the flame is rich in CO, which is a species produced by combustion. Among the four curves, the best curve that approves the CO reduction is characterized by the air inlet temperature T=750 K in the two considered cases. In the first case defined by x/R=0.14, it has been noted that the extremum of the curve corresponds to a mass fraction of the CO equal to Yco=0.23 which is located in the position defined by r/R=0.55. In the second case defined by x/R=0.38, the extremum of the curve corresponds to a mass fraction of the CO equal to Yco=0.22 which is located in the position defined by r/R=0.55. According to these results, it has been observed that the maximum value of the CO mass fraction appears near the axis. Elsewhere, it presents a very weak value, particularly near the lateral surface. Indeed, it has been observed that the CO profiles present the same tendency with the temperature, since the CO is produced by the combustion of CH_4 found in G27.

Table 1 presents the values of the mass fraction of carbon monoxide for the incoming air temperature T=300K, T=500K, T=750K and T=900K in the station x/R= 0.14 while the table 2 represents the station x/R=0.38.

Table 1: The values of the CO mass fraction for the station x/R= 0.14.
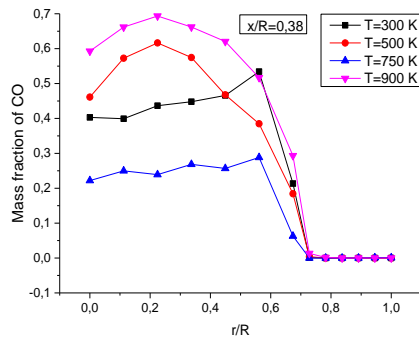
Yco	r/R=0.0	r/R=0.2	r/R=0.4	r/R=0.6
T=300 K	0.18	0.17	0.25	0.38
T=500 K	0.24	0.55	0.57	0.23
T=750 K	0.09	0.10	0.085	0.22
T=900 K	0.35	0.45	0.50	0.24

Table 2: The values of the CO mass fraction for the station x/R= 0.38.

Yco	r/R=0.0	r/R=0.2	r/R=0.4	r/R=0.6
T=300 K	0.40	0.41	0.42	0.36
T=500 K	0.45	0.58	0.53	0.26
T=750 K	0.21	0.23	0.235	0.16
T=900 K	0.58	0.67	0.64	0.27
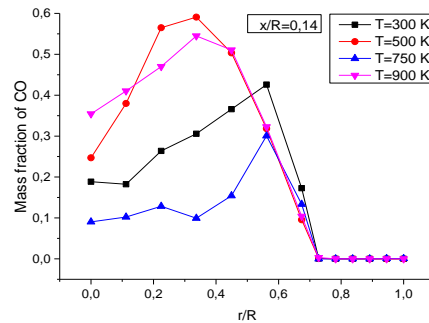
(a) x/R=0.14

(b) x/R=0.38

Figure 5. *Radial profiles of the CO mass fraction*

VI. Conclusion

This paper presents a numerical simulation using the CFD code FLUENT to study the preheating effect of air in a non-premixed combustion chamber fed with a G27 fuel. Under these conditions, the phenomenon of preheating the injected air with the fuel G27 initially subjected to a constant temperature equal to T=300 K was investigated. Moreover, several cases are considered defined by the air inlet temperatures equal to T=300 K, T=500 K, T=750 K and T=900 K.

The different results obtained make it possible to draw the following conclusions:

• Combustion with less appropriate energy loss the air temperature equal to T=750 K given by the temperature of the fuel equal to T=300 K.

• The inlet conditions characterized by air temperature T=750 K reduce the emission of carbon monoxide CO in combustion emissions that are harmful to the environment, where the temperature of the fuel is equal T=300 K.

VII. Nomenclature

R	Constant of ideal gas	$[J.kg^{-1}.K^{-1}]$
R, r	Radius	$[m]$
T	Temperature	$[K]$
u	Axial velocity	$[m.s^{-1}]$
x	Cartesian coordinate	$[m]$
y	Mass fraction of chemical species	$[\%]$
	Greeks symbols	
α	Thermal Diffusivity	$[m^2.s^{-1}]$
ρ	Density	$[kg.m^{-3}]$
ε	Dissipation of energy	$[m^2.s^{-3}]$
ω	Arrhenius terms	$[s^{-1}]$
λ	Thermal conductivity	$[kW.m^{-1}.K^{-1}]$
μ	Chemical potential, Viscosity	$[kg.m^{-1}.s^{-1}]$
N	Number of chemical species	
	Indices	
i,j,k	Indices of Cartesian coordinate	

IX. References

1. International Energy Agency Report, DOE 0484 (2007) EIA, 2007.
2. Masters, J.; Webb, R.J.; Davies, R.M. Use of modelling techniques in the design and application of recuperative burners. *Journal of the Institute of Energy* 52 (413) (1979) 196-205.
3. Rasani, M.R.; Aldlemy, M.S.; Harun, Z. Fluid-structure interaction analysis of rear spoiler vibration for energy harvesting potential. *Journal of Mechanical Engineering and Sciences* 11(1) (2017) 2415-2424.
4. Atia, A.; Mohammedi, K. State of the art on enhanced oil recovery with CO_2 sequestration for low carbon industry. *Algerian Journal of Environmental Science and Technology* 3 (2017) 5-8.
5. Tahseen, T.A.; Ishak, M.; Rahman, M.M. A numerical study of forced convection heat transfer over a series of flat tubes between parallel plates. *Journal of Mechanical Engineering and Sciences* 3 (2012) 271-280.
6. Reda, E; Zulkifli, R.; Harun, Z. Large eddy simulation of wind flow through an urban environment in its full-scale wind tunnel models. *Journal of Mechanical Engineering and Sciences* 11 (2) (2017) 2665-2679.
7. Boukhari, A.; Bessaïh, R. Numerical heat and mass transfer investigation of hydrogen absorption in an annulus-disc reactor. *International journal of Hydrogen energy* 40 (2015) 13708-13718.
8. Milani, A.; Saponaro, A. Diluted combustion technologies. *IFRF (International Flame Research Foundation) Combustion Journal* Article n° 200101, Février 2001.
9. Katsuki, M.; Hasegawa, T. The science and technology of combustion in highly preheated air. *Proceeding of the Combustion Institute* 27 (1998) 3135-3145.
10. Bouras, F.; Attia, M.E.H.; Khaldi, F.; SI-AMEUR, M. Control of the Methane Flame Behavior by the Hydrogen Fuel Addition: Application to Power Plant Combustion Chamber . *International journal of Hydrogen energy* 42 (13) (2017) 8932-8940.
11. Bouras, F.; Soudani, A.; Si Ameur, M. Beta-PDF Approach for Large Eddy Simulation of Non-premixed Turbulent Combustion.*International Review of Mechanics Engineering* 4 (2010) 1096-1100.
12. Pierce, C.P.; Moin, P. Progress-Variable Approach for Large-Eddy Simulation of Non-Premixed Turbulent Combustion . *Journal of Fluid Mechanics* 504 (2004) 73-98.
13. Bouras, F.; Attia, M.E.H.; Khaldi, F. Entropy Generation Optimization in Internal Combustion Engine *Environmental Processes* 2 (2) (2015) 233-243.
14. Bouras, F.; Soudani, A.; Si Ameur, M. Large Eddy Simulation for Lean Premixed Combustion *Canadian. Journal of Chemical Engineerin* 91 (2013) 231-238.

15. Attia, M.E.H.; Driss, Z.; Khechekhouche, A. Numerical Study of the Combustion of CH$_4$-C$_3$H$_8$/Air: Application to a Combustion Chamber with Two Coaxial Jets. *International Journal of Energetica (IJECA)* 2 (2) (2017) 38-43.

16. Attia, M.E.H.; Khechekhouche, A.; Driss, Z. Numerical Simulation of Methane-Hydrogen Combustion in the Air: Influence on Combustion Parameters. *Indian Journal of Science and Technology* 11 (2) (2018) 1-8.

Please cite this Article as:
 Boukhari A., Attia M.E.H., Driss Z *.,Reduction of CO Emissions in the Environment by Preheating the Air in a Combustion Chamber,* **Algerian J. Env. Sc. Technology**, **5**:1 **(2019) 852-857**